Supplement of The Cryosphere, 13, 545–556, 2019
https://doi.org/10.5194/tc-13-545-2019-supplement

The Cryosphere
Open Access

Supplement of

Past and future dynamics of the Brunt Ice Shelf from seabed bathymetry and ice shelf geometry

Dominic A. Hodgson et al.

Correspondence to: Dominic A. Hodgson (daho@bas.ac.uk)

1. Estimation of sub-ice shelf bathymetry from gravity

Bathymetry under ice shelves is critical for understanding their long-term stability, but is hard to determine. Radar techniques do not penetrate the water column, seismic measurements are time consuming with many areas inaccessible, and direct observation using autonomous underwater vehicles, such as NERC's Boaty Mc Boat Face, is risky and only provide a narrow swath of data. An alternative approach is to use gravity signals, collected rapidly and efficiently with airborne systems, to invert for sub-ice shelf bathymetry. Inversion of gravity data relies on the density contrast between water and the underlying rock, which can provide a clear bathymetric signal. Inversion of gravity data for sub-ice or sub-marine topography has been applied since the early surveys of Antarctica in the 1960's (Bentley, 1964), and continues to be applied in both marine and terrestrial settings to this day (Cochran and Bell, 2012; Fretwell et al., 2013; Sandwell and Smith, 1997). However, it has been shown that some of these inversions provided poor estimates of sub-ice shelf topography (Brisbourne et al., 2014). Such inaccuracies in bathymetry derived from gravity data likely reflect un-modelled sub-surface geological features, which can distort the gravity field, and may have a similar wavelength to the desired bathymetric signal. Despite these limitations, gravity data can provide an important first look at sub-ice shelf bathymetry when other data is limited, or lacking.

To provide the most robust estimate of sub-ice topography we have developed a four-stage process to derive sub-ice shelf topography from gravity data, while maintaining close correspondence to available direct bathymetric observations (Supplementary Fig. 1). The detailed steps for calculating the final gravity improved topography are described below. We note that this is not a formal inversion, but rather a repeatable procedure (algorithm) for estimating sub-ice shelf bathymetry from gravity data constrained by sparse direct (swath/seismic/radar) observations.

Step 1. Initiate. The 3D gravity effect of the initial known topography, interpolated from radar, seismic and swath bathymetry measurements, is calculated. This Bouguer correction is subtracted from the observed grid of free air gravity anomalies. The resulting Bouguer anomaly contains signals caused by variations in crustal thickness, shallow geological bodies with distinct densities, and errors in the input topographic data.

Step 2. Isolate. The long wavelength gravity anomaly, assumed to be due to crustal thickness variation, is isolated using a low pass filter. This long wavelength anomaly is subtracted from the Bouguer anomaly, leaving the 1st residual gravity anomaly, which contains signatures due to shallow geological bodies with distinct densities, and errors in the input topographic data. If distinct geological features can be recognised 3D models of their gravity signatures are calculated and subtracted leaving the 2nd residual gravity anomaly, theoretically only due to errors in the input topographic data.

Step 3. Calculate. The 2nd residual gravity anomaly is converted from mGal to equivalent rock thickness using the Bouguer slab formula, assuming a density of 2.67 and 1.028 gcm^{-3} for rock and water respectively. This equivalent topographic correction is added back to the initial topography to provide the 1st estimate of gravity improved topography.

Step 4. Constrain. Discrepancies between the 1st estimate of sub-ice shelf topography and the direct point observations of topography relate to un-modelled geological factors, and features resolved by higher resolution topographic datasets. We interpolate this error field between the points where topography is well constrained to provide a residual topographic correction across the study area. This is added to the 1st estimate of gravity improved topography to provide the final blended gravity improved topography estimate.

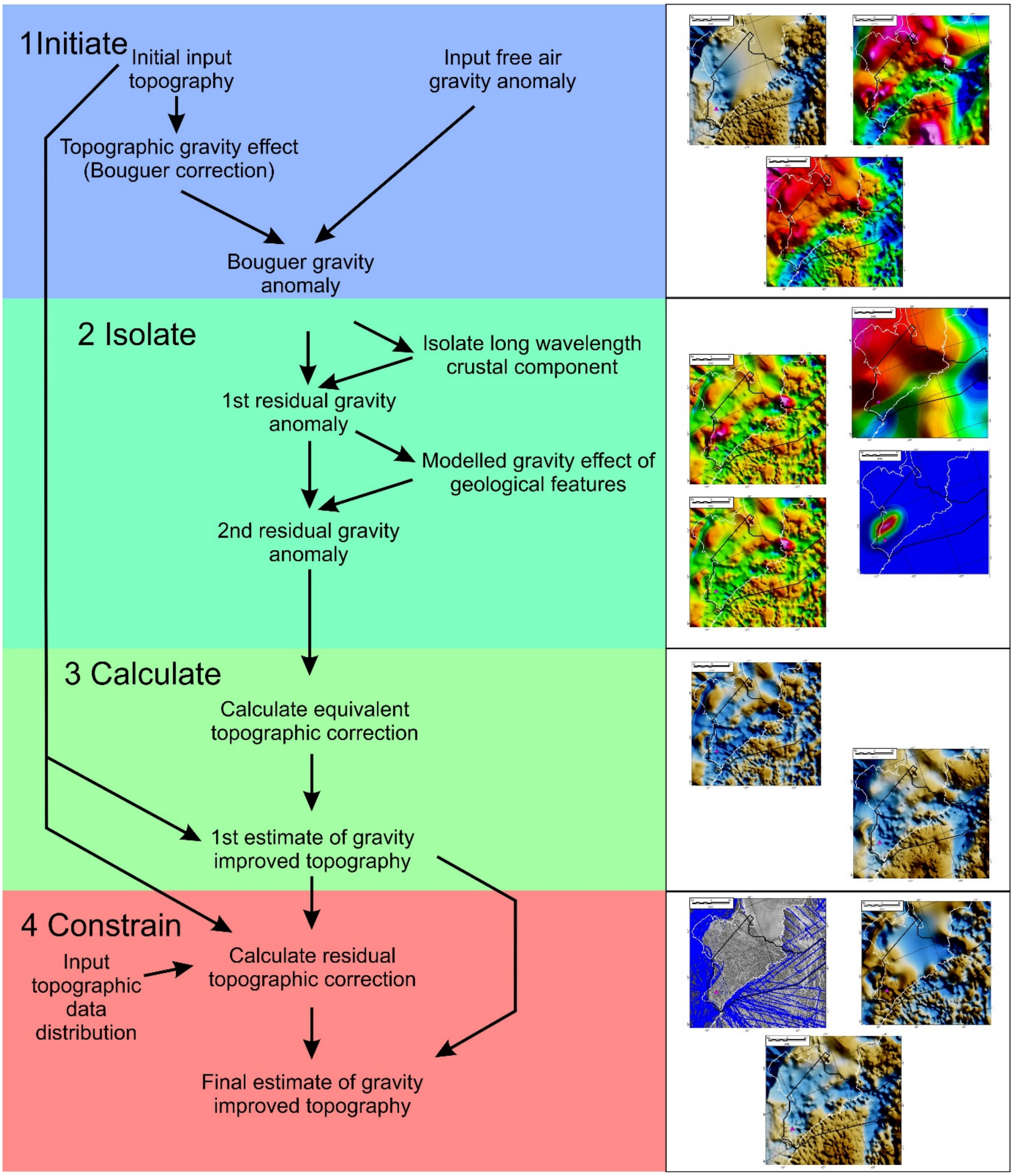

Supplementary Figure 1. Flow diagram showing recovery of bathymetry from gravity. Right-hand panel shows example grids at each stage (red-green-pink colours = gravity (mGal), blue-brown colours = topography (m)). Note Pink triangle marks original Halley VI site.

Specific notes for this study:

The Bouguer correction was calculated using a 3D Gauss-Legendre quadrature (GLQ) method (von Frese et al., 1981), assuming a uniform observation altitude of 450 m, coincident with the 2017 survey altitude over the ice shelf. Results are therefore not valid onshore where surface elevations are above 450 m. Standard densities for the Bouguer correction of 915, 1028 and 2670 kg m^{-3} for ice, water and rock respectively were used.

The residual crustal anomaly was isolated using a 150 km low pass Gaussian filter. This appeared to remove any linear regional trend in the observed gravity anomaly, suggesting the long wavelength signal due to the extreme change in crustal thickness between the East Antarctic continent and the oceanic crust of the Weddell Sea have been accounted for.

For areas outside the high-resolution 2017 data anomalies appear in the Bouguer gravity field which are likely artefacts of the low resolution of the reconnaissance free air gravity data.

The underlying gravity data set is described and analysed in more detail in (Jordan and Becker, 2018) and the associated gravity data is published through the UK polar data centre (Becker et al., 2018).

2. Comparison of gravity improved topographic estimate and aeromagnetic data

Aeromagnetic data across the study area shows a clear high frequency signal beneath the main survey area. This suggests the geological basement is close to the surface (Supplementary Fig. 2).

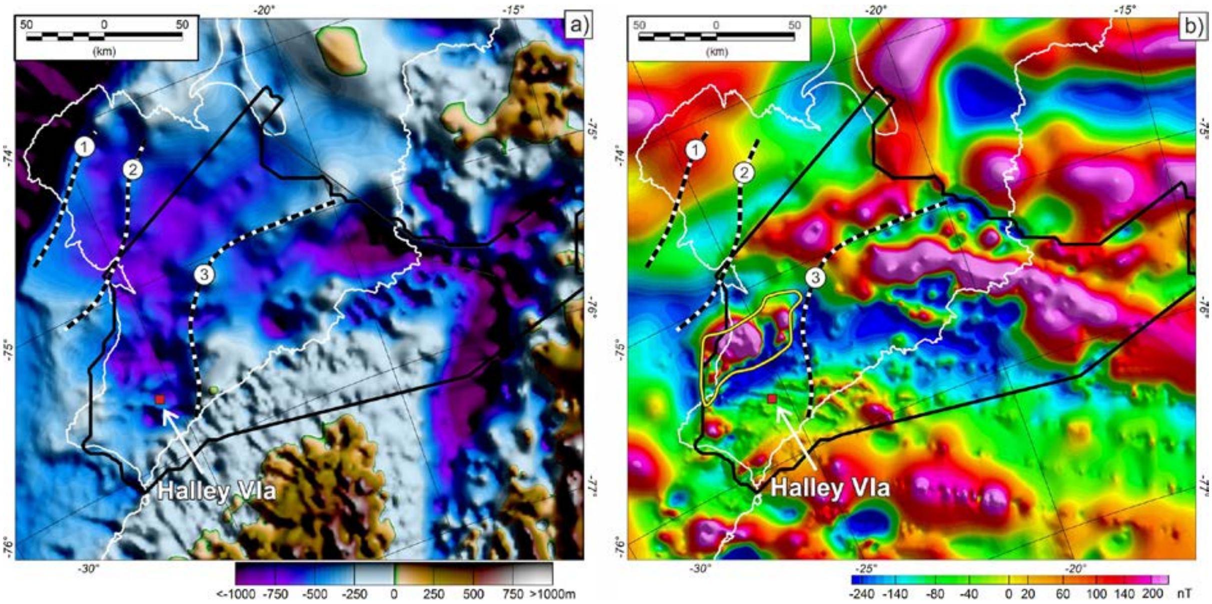

Supplementary Figure 2. Comparison of topography and aeromagnetic data. a) Final estimate of gravity improved topography. Note black and white dashed lines (1-3) marking potential former grounding lines which likely acted as pinning points. Solid black outline marks edge of 2017 gravity survey where gravity derived topography is most robust. Red square marks Halley VIa site. b) Aeromagnetic data (Jordan and Becker, 2018; Jordan et al., 2018) over the study area. A direct regional correlation between topography and the underlying geological structures revealed by the magnetic data cannot be made, indicating the bathymetric signal likely dominates the geological signal. However, local correlations can be seen, for example between the northern part of ridge 3 and a linear magnetic low. Such correlation suggests that subglacial geology is influencing the bathymetry, but relatively sparse data coverage makes more detailed analysis difficult. Note yellow outline marks gravity high (Fig. 4b in main text) associated with very high amplitude magnetic anomalies (>1000 nT) attributed to a mafic intrusion (Jordan and Becker, 2018).

References

Becker, D., Jordan, T.A., Corr, H., Robinson, C., 2018. Strapdown gravity survey across the Brunt Ice Shelf (2017) UK Polar Data Center https://doi.org/10.5285/79e63097-f5dc-41ff-8ca5-36bc4f95a6ff.

Bentley, C., 1964. The structure of Antarctica and its ice cover, in: Odishaw, H. (Ed.), Research in Geophysics Vol. 2, Solid Earth and Interface Phenomena. MIT Press, Cambridge, Mass., pp. 335–389.

Brisbourne, A.M., Smith, A.M., King, E.C., Nicholls, K.W., Holland, P.R., Makinson, K., 2014. Seabed topography beneath Larsen C Ice Shelf from seismic soundings. The Cryosphere 8, 1-13.

Cochran, J.R., Bell, R.E., 2012. Inversion of IceBridge gravity data for continental shelf bathymetry beneath the Larsen Ice Shelf, Antarctica. Journal of Glaciology 58, 540-552, https://doi.org/10.3189/2012JoG11J033.

Fretwell, P., Pritchard, H.D., Vaughan, D.G., Bamber, J., Barrand, N., Bell, R., Bianchi, C., Bingham, R., Blankenship, D., Casassa, G., Callens, D., Conway, H., Cook, A.J., Corr, H.F.J., Damaske, D., Damm, V., Ferraccioli, F., Forsberg, R., Fujita, S., Gogineni, P., Griggs, J.A., Hindmarsh, R., Holmlund, P., Holt, J.W., Jacobel, R.W., Jenkins, A., Jokat, W., Jordan, T.A., King, E.C., Kohler, J., Krabill, W., Riger-Kusk, R., Langley, K.A., Leitchenkov, G., Leuschen, C., Luyendyk, B.P., Matsuoka, K., Nogi, Y., Nost, O.A., Popov, S., Rignot, E., Rippin, D.M., Riviera, A., Roberts, J., Ross, N., Siegert, M.J., Smith, A.M., Steinhage, D., Studinger, M., Sun, B., Tinto, B.K., Welch, B.C., Young, D.A., Xiangbin, C., Zirizzotti, A., 2013. Bedmap2: improved ice bed, surface and thickness datasets for Antarctica. The Cryosphere 7.

Jordan, T.A., Becker, D., 2018. Investigating the distribution of magmatism at the onset of Gondwana breakup with novel strapdown gravity and aeromagnetic data. Physics of the Earth and Planetary Interiors 282, 77-88, https://doi.org/10.1016/j.pepi.2018.1007.1007.

Jordan, T.A., Corr, H., Robinson, C., 2018. Aeromagnetic survey across the Brunt Ice Shelf (2017) UK Polar Data Center https://doi.org/10.5285/410ee2f9-2d22-4155-aaed-43b93a7c3d62.

Sandwell, D.T., Smith, W.H.F., 1997. Marine gravity anomaly from Geosat and ERS 1 satellite altimetry Journal of Geophysical Research 102, 10039-10054.

von Frese, R.R.B., Hinze, W.J., Braile, L.W., Luca, A.J., 1981. Spherical earth gravity and magnetic anomaly modeling by Gauss- Legendre quadrature integration. Journal of Geophysics 49, 234-242.